Structure of the IIA Domain of the Glucose Permease of *Bacillus subtilis* at 2.2-Å Resolution†,‡

Der-Ing Liao,§ Geeta Kapadia,§ Prasad Reddy,∥ Milton H. Saier, Jr.,⊥ Jonathan Reizer,⊥ and Osnat Herzberg*,§

Center for Advanced Research in Biotechnology, Maryland Biotechnology Institute, University of Maryland, 9600 Gudelsky Drive, Rockville, Maryland 20850, Center for Advanced Research in Biotechnology, National Institute of Standards and Technology, 9600 Gudelsky Drive, Rockville, Maryland 20850, and Department of Biology, University of California at San Diego, La Jolla, California 92093-0116

Received June 3, 1991; Revised Manuscript Received July 31, 1991

ABSTRACT: The crystal structure of the IIA domain of the glucose permease of the phosphoenolpyruvate:sugar phosphotransferase system (PTS) from *Bacillus subtilis* has been determined at 2.2-Å resolution. Refinement of the structure is in progress, and the current *R*-factor is 0.201 ($R = \sum_h||F_o| - |F_c||/\sum_h|F_o|$, where $|F_o|$ and $|F_c|$ are the observed and calculated structure factor amplitudes, respectively) for data between 6.0- and 2.2-Å resolution for which $F \geq 2\sigma(F)$. This is an antiparallel β-barrel structure that incorporates "Greek key" and "jellyroll" topological motifs. A shallow depression is formed at the active site by part of the β-sheet and an Ω-loop flanking one side of the sheet. His83, the histidyl residue which is the phosphorylation target of HPr and which transfers the phosphoryl group to the IIB domain of the permease, is located at the C-terminus of a β-strand. The N^{ϵ} atom is partially solvated and also interacts with the N^{ϵ} atom of a second histidyl residue, His68, located at the N-terminus of an adjacent β-strand, suggesting they share a proton. The geometry of the hydrogen bond is imperfect, though. Electrostatic interactions with other polar groups and van der Waals contacts with the side chains of two flanking phenylalanine residues assure the precise orientation of the imidazole rings. The hydrophobic nature of the surface around the His83–His68 pair may be required for protein–protein recognition by HPr or/and by the IIB domain of the permease. The side chains of two aspartyl residues, Asp31 and Asp87, are oriented toward each other across a narrow groove, about 7 Å from the active-site His83, suggesting they may play a role in protein–protein interaction. A model of the phosphorylated form of the molecule is proposed, in which oxygen atoms of the phosphoryl group interact with the side chain of His68 and with the main-chain nitrogen atom of a neighboring residue, Val89. The model, in conjunction with previously reported site-directed mutagenesis experiments, suggests that the phosphorylation of His83 may be accompanied by the protonation of His68. This may be important for the interaction with the IIB domain of the permease and/or play a catalytic role in the phosphoryl transfer from IIA to IIB.

The phosphoenolpyruvate:sugar phosphotransferase system (PTS) first described by Kundig et al. (1964) is a permease-mediated transmembrane carbohydrate transport system unique to bacteria. It also regulates the uptake of some PTS and non-PTS sugars via various mechanisms [for reviews see Postma and Lengeler (1985), Reizer et al. (1988), Saier (1985), and Meadow et al. (1990)]. The system consists of two general energy-coupling components, Enzyme I and a heat-stable phosphocarrier protein (HPr), and sugar-specific permeases, Enzymes II, which typically consist of three domains, IIA, IIB, and IIC. A characteristic feature of the PTS is the tight coupling of sugar transport to phosphorylation. The phosphoryl group is derived from phosphoenolpyruvate (PEP) and is transferred to the sugar via a chain of four phosphorylated PTS protein intermediates: phospho-Enzyme I, phospho-HPr, phospho-Enzyme IIA, and phospho-Enzyme IIB. The phosphorylation of Enzyme IIB leads to the opening of a channel such that the translocation of the sugar across the cytoplasmic membrane occurs. The three domains of the PTS permeases (approximate total molecular mass of 68 kDa) may be fused together in a single polypeptide chain or can exist in two or three distinct polypeptide chains (Saier & Reizer, 1990). In this nomenclature, the IIA proteins correspond to the proteins of the PTS which have previously been designated Enzymes III or Factors III.

The *Bacillus subtilis* glucose permease consists of a single polypeptide chain with the domain order IICBA (Gonzy-Treboul et al., 1989; Sutrina et al., 1990). The IIA domain is linked to the IICB domains via a hydrophilic polypeptide segment denoted the Q-linker (Wootton & Drummond, 1989), which is thought to be structurally flexible. The IIA domain of the glucose permease has been shown to stimulate the phosphorylation of sucrose, suggesting that the IIA^{glc} domain of *B. subtilis* can also interact and phosphorylate the sucrose permease (Sutrina et al., 1990; J. Reizer et al., 1991).

The IIA^{glc} domain has been overexpressed and purified as a soluble protein which contains 13 of the 34 amino acid residues that have been proposed to comprise the interdomain Q-linker (Sutrina et al., 1990). This is a small protein of 162 amino acid residues of which 41% are identical to those of the *Escherichia coli* IIA^{glc} (Enzyme III^{glc}). For overexpression, the N-terminal valine residue was replaced by a methionine. The protein is active both in vivo and in vitro and can thus be phosphorylated by HPr and transfer its phosphoryl group to the IIB domain (J. Reizer et al., 1991). It has been shown to complement the glucose fermentation defect of a *crr* mu-

† Supported by National Science Foundation Grant DMB 9019340 to O.H.

‡ The coordinates for this structure have been deposited in the Brookhaven Protein Data Bank.

* Corresponding author.
§ University of Maryland.
∥ National Institute of Standards and Technology.
⊥ University of California at San Diego.

0006-2960/91/0430-9583$02.50/0

Table I: Enzyme IIA^{glc} Data Processing Statistics

shell lower limit (Å)	no. of rflcns possible	no. of rflcns missing	no. of observns	$\langle I/\sigma(I)\rangle$	fraction with $I \geq 2\sigma(I)$	R_{sym}[a]
4.03	1263	5	4140	68.2	0.98	0.033
3.20	1200	0	3678	47.6	0.97	0.043
2.79	1172	8	3422	26.4	0.94	0.064
2.54	1183	46	3187	16.3	0.89	0.096
2.35	1174	115	2699	12.4	0.86	0.108
2.22	1143	538	872	7.7	0.79	0.131
total	7135	712	17998	33.0	0.92	0.046
Absolute Scaling						
overall scale				0.072		
overall temperature factor				25.6 Å^2		

[a] $R_{sym} = \sum_h \sum_i |\langle I\rangle - I(h)_i| / \sum_h \sum_i I(h)_i$ for symmetry-related observations; h = Miller indices, I = intensity.

tation in *E. coli* (Gonzy-Treboul & Steinmetz, 1987) and is capable of replacing the IIA^{glc} of *E. coli* in regulating the non-PTS maltose transport (Dean et al., 1990), as well as the *E. coli* lactose and melibiose permeases, glycerol kinase, and adenylate cyclase (J. Reizer et al., 1991). Phosphorylation of the *E. coli* protein occurs on the N$^{\epsilon}$ position of His90 (Dörschug et al., 1984). The equivalent position in the recombinant *B. subtilis* IIA^{glc} is His83.

Since the three intermediate steps of phosphoryl transfer via the PTS involve protein–protein interactions, it is expected that the assisting machinery of each such transfer reaction comprises residues from both proteins. The determination of the three-dimensional structures of all of these proteins should help reveal these modes of interactions and the molecular events associated with the process. We have previously reported the crystallization of the *B. subtilis* HPr (Kapadia et al., 1990) and of the *B. subtilis* IIA domain of the glucose permease (Kapadia et al., 1991). Other structural studies on HPr include X-ray and nuclear magnetic resonance (NMR) work on *E. coli* HPr (El-Kabbani et al., 1987; Klevit & Waygood, 1986) and NMR work on the *B. subtilis* HPr (Wittekind et al., 1989, 1990). The NMR and previous X-ray structures of HPr do not corroborate each other. Other structural studies of IIA domains are also in progress. These include X-ray work on the fast form of Enzyme III^{glc} from *E. coli* (J. Remington, personal communication) and on the N-terminal domain of the phosphorylating subunit of the mannose permease from *E. coli* (Gênovésio-Taverne et al., 1990), whose sequence is not related to the above two IIA domains. A secondary structure assignment based on NMR has been reported for the *E. coli* Enzyme III^{glc} (Pelton et al., 1991) and for the *B. subtilis* IIA^{glc} domain (Fairbrother et al., 1991).

We present here the X-ray crystal structure determination of the IIA domain of the glucose permease from *B. subtilis* at 2.2-Å resolution. The structure is sufficiently reliable to describe it in atomic detail. It shows the precise conformation of the key histidyl residue and its interactions with neighboring residues. The architecture of the active site, in the context of other biochemical data, indicates which of the amino acid residues may play a role in protein–protein recognition and/or phosphoryl transfer. A model of the phosphorylated state of the protein has been built on the basis of this unphosphorylated X-ray structure.

Experimental Procedures

(*a*) *Protein Purification and Crystallization.* The protocol for the overproduction and purification of the IIA domain of the glucose permease of *B. subtilis* will be described elsewhere (Reizer et al., unpublished data). Crystals were obtained in 57–62% saturated ammonium sulfate solution, 0.5% (w/v) poly(ethylene glycol) 1000, and 100 mM phosphate buffer at pH 8.0, as described previously (Kapadia et al., 1991). The crystals are orthorhombic, with space group $C222_1$ and unit cell dimensions of a = 74.2 Å, b = 54.9 Å, and c = 67.0 Å. They diffract to at least 1.8-Å resolution.

(*b*) *Structure Determination.* The structure was determined by using the well-established multiple isomorphous replacement method (MIR) and improving the phases by solvent-flattening techniques. X-ray intensity data to 2.2-Å resolution for the native protein and to 2.8-Å resolution for three heavy-atom derivatives were collected on a Siemens area detector mounted on a Siemens three-axis goniostat. Graphite monochromated CuKα X-rays were generated with a Rigaku Rotaflex RU-200BH rotating anode source. The data were processed with the computer program suite XENGEN (Howard et al., 1987). The structure factors of the native data were scaled to absolute values with the computer program ORESTES, written by W. E. Thiessen and H. A. Levy. The statistics of the data processing for the native set are given in Table I.

The MIR and solvent-flattening work was carried out using the computer program suite PHASES (Furey & Swaminathan, 1990). Heavy-atom binding sites were determined from difference Patterson maps and difference Fourier maps in the usual manner (Blundell & Johnson, 1976). The positional parameters and occupancies of the heavy atoms were refined by lack of closure error minimization (Dickerson et al., 1968). Some statistics for the heavy-atom derivatives are given in Table II. In fact, only the uranyl derivative data was of sufficiently high quality to be used at 2.8-Å resolution. The other two platinum derivatives were useful only at 5-Å resolution. The absolute hand was determined using the anomalous data of the uranyl derivative as described before (Blundell & Johnson, 1976), and the anomalous signal was included in the phasing as well. A phase set was obtained with a mean figure of merit of 0.635. A 2.8-Å resolution electron density map was computed with centroid phases (Blow & Crick, 1959) and measured structure factor amplitudes weighted by the figure of merit. The map showed the contrast between protein and solvent and continuous stretches of density consistent with

Table II: Heavy-Atom Derivative Statistics

compound[a]	soaking time (days)	R_{iso}[b] (2.8 Å)	resolution used (Å)	no. of unique reflections used	no. of sites	R_{cen}[b]	$\langle f_H\rangle/\langle E_H\rangle$[b]
5 mM uranyl acetate	4	0.265	2.8	3051	3	0.450	3.09
1 mM platinum ethylenediaminodichloride	2	0.122	5.0	655	2	0.532	1.77
2 mM chloro-(2,2′:6,2″-terpyridine)platinum(II)	4	0.251	5.0	620	2	0.521	2.00

[a] All the soaking experiments were done in 100 mM Tris–acetate, pH 6.0, and 72% saturated ammonium sulfate. [b] $R_{iso} = \sum_h ||F_{PH}obs| - |F_P obs||/\sum F_P obs|$. $R_{cen} = \sum_{h\,centric}||F_{PH}obs| - |F_P obs + F_H calc||/\sum_{h\,centric}||F_{PH}obs| - |F_P obs||$. h = Miller indices; obs = observed; calc = calculated; F_P, F_{PH}, F_H = native protein, derivative protein, and heavy-atom structure factors, respectively. $\langle E_H\rangle$, rms lack of closure error; $\langle f_H\rangle$, rms heavy atom scattering.

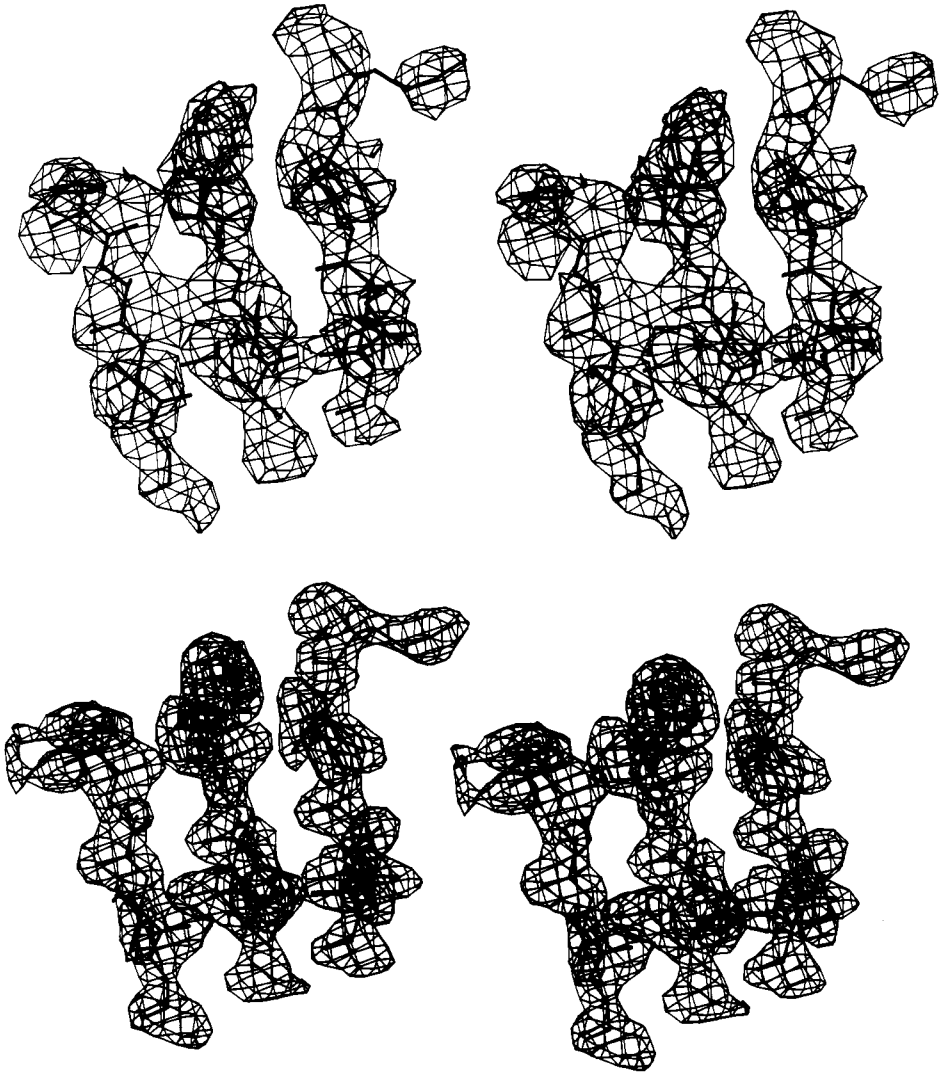

FIGURE 1: Stereoscopic view of a region of the electron density map in the vicinity of the active-site His83. Segments of three β-strands are shown from left to right: His68–Gly71, Leu81–Phe84, and Met128–Val132. (Top) The 2.8-Å solvent-flattened MIR map. (Bottom) The 2.2-Å map with calculated phases and the coefficient $2F_o - F_c$.

β-strands. However, this map was rather noisy and difficult to interpret.

Although the volume occupied by solvent in these crystals is rather low (~40%), solvent flattening (Schevitz et al., 1981; Wang, 1985) proved useful in improving the map. The procedure was carried out in reciprocal space, as implemented in PHASES. The solvent content was specified for masking purposes as only 35%. After each step of mask calculation, four cycles of map modification, map inversion, and phase combination with the MIR phases were carried out. A total of four such solvent-flattening steps were performed. The average cumulative phase shift from the initial MIR phases was 39.6°. The figure of merit was 0.85. This value should be considered as a measure of convergence and not as indication of the quality of the phases. In spite of the low solvent content, the improvement of the phases was sufficient to enable unambiguous tracing of the polypeptide chain consistent with the known amino acid sequence. Figure 1 (top) shows a region of the map around the active-site histidyl residue.

A molecular model was fitted to the electron density map on the E&S PS390 interactive graphics system with the program FRODO (Jones, 1982). This initial model consisted of all but the first 11 amino acid residues and the C-terminal residue. The electron density associated with these was difficult to interpret.

(*c*) *Structure Refinement.* The molecular dynamics refinement program X-PLOR was used to refine the structure (Brünger et al., 1987). Data between 6.0 and 2.2 Å for which $F \geq 2\sigma(F)$ have been refined, using the simulated annealing slow cooling protocol as described in the program manual: First, 160 steps of energy minimization with restraints to the X-ray data were carried out using the Powell conjugate gradient minimizer (Powell, 1977). The α-carbon atom positions were constrained to their initial position in this step and an overall temperature factor of 25.6 Å^2 was used, based on the estimated value from the scaling of the data to absolute scale. This reduced the R-factor from 0.473 to 0.327 ($R = \sum_h ||F_o| - |F_c|| / \sum_h |F_o|$, where $|F_o|$ and $|F_c|$ are the observed and calculated structure factor amplitudes, respectively). The dynamics step was then invoked, heating the system to 3000 K. The temperature was reduced in increments of 25 K, carrying out 50 steps of integration in each range, until the system had cooled down to 300 K. The resulting R-factor at the end of the dynamics was 0.280. This was followed by group and individual temperature-factor refinement, reducing the R-factor further to 0.250.

After each cycle of X-PLOR refinement, the model was displayed on the interactive graphic system with two types of electron density maps: (1) a map computed with the coefficients $2|F_o| - |F_c|$ and calculated phases and (2) a map with

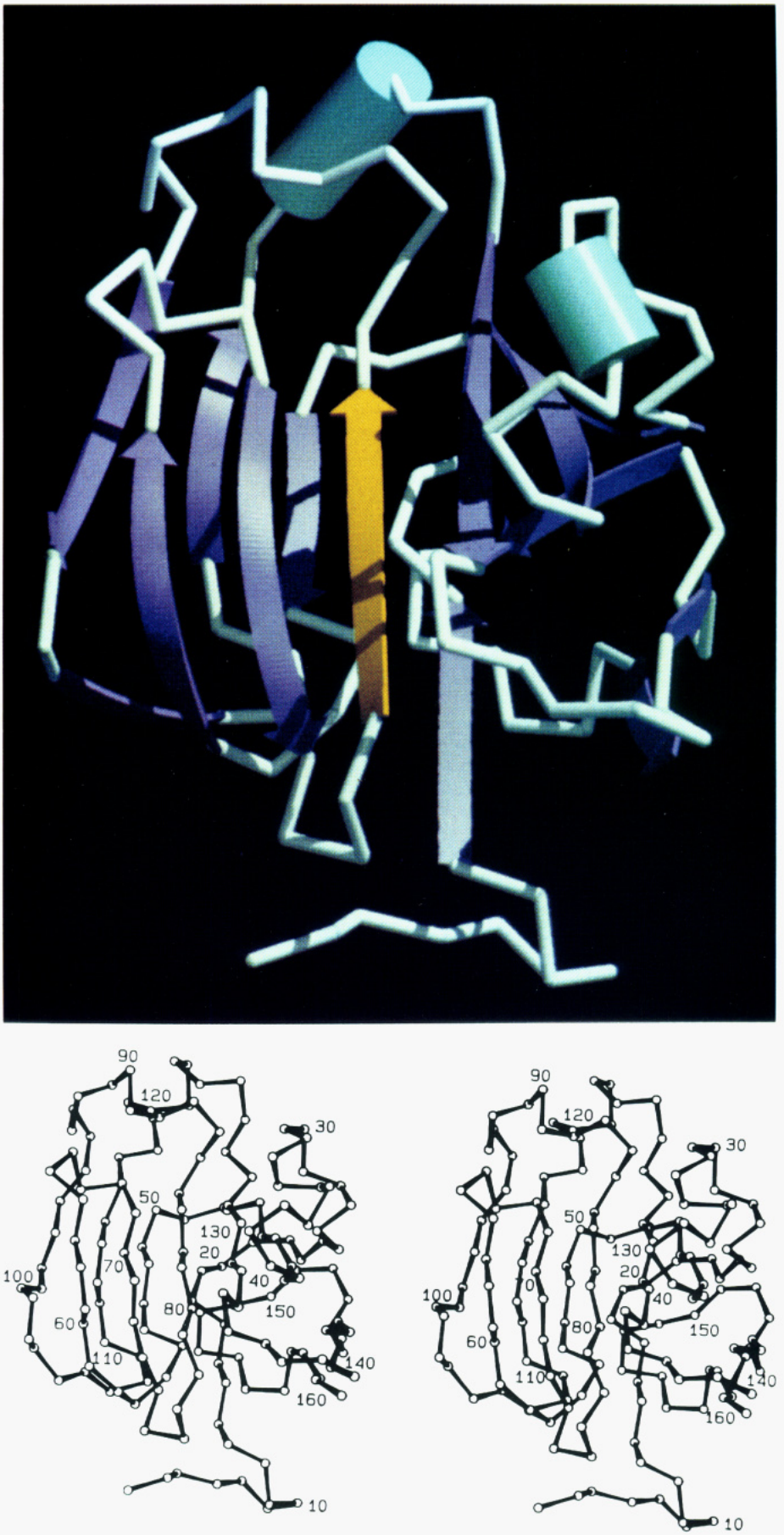

FIGURE 2: Fold of the IIA^{glc} from *B. subtilis*. (Top) The overall fold, highlighting secondary structure motifs: β-strands are shown as ribbons, helices (longer than four residues) as cylinders. The active-site His83 is located at the C-terminus of the golden β-strand. The model was generated on a Silicon Graphics Iris/4D workstation with the computer program RASTER3D written by David Bacon. (Bottom) Stereoscopic representation showing the α-carbon positions in the molecule. Every tenth amino acid is labeled.

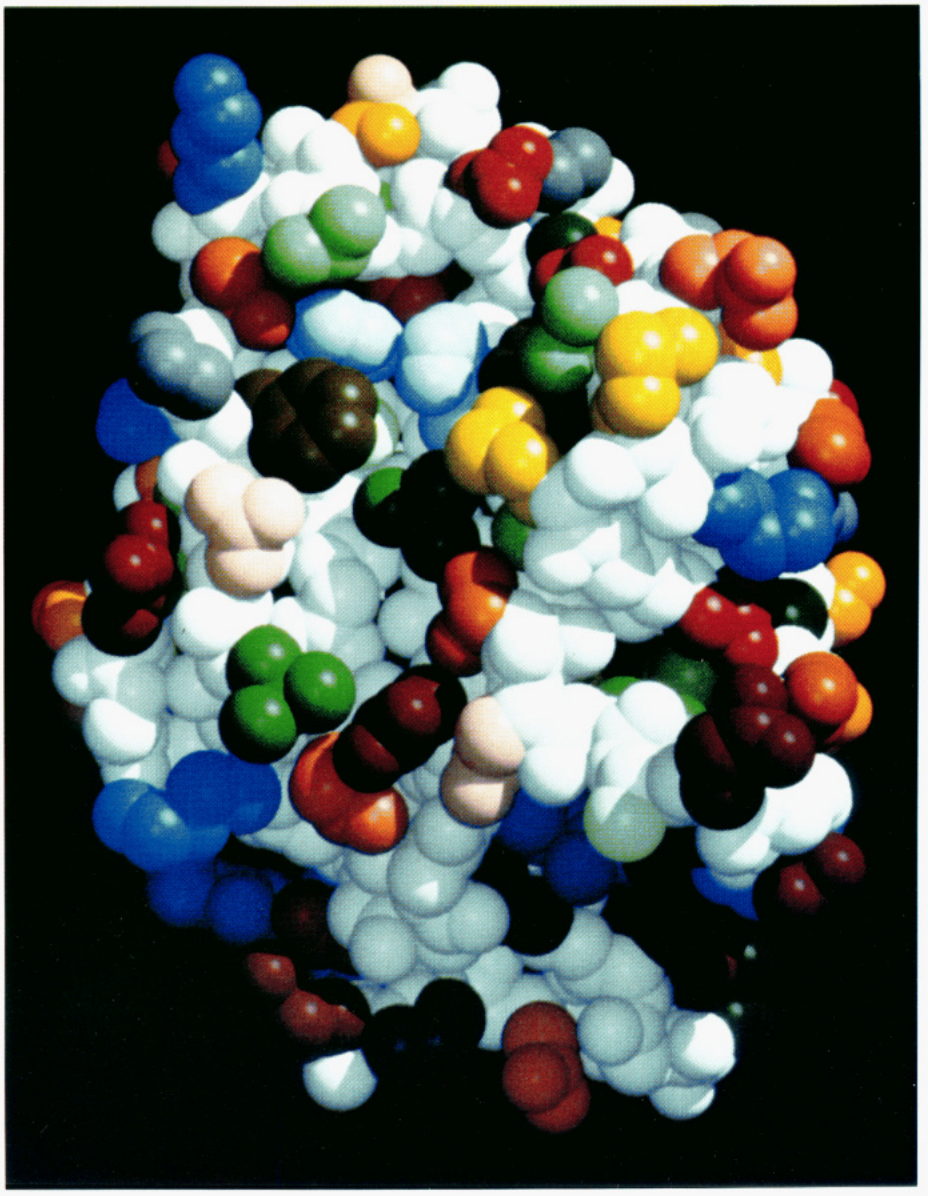

FIGURE 3: Computer-generated space-filling model of the IIA^{glc} molecule. The orientation is the same as in Figure 2. Main-chain atoms are white, aliphatic side chains are green, prolines are gray, aromatic side chains are brown, and polar side chains are pink and orange. Negatively charged residues are red, and positively charged ones are blue. The darker the color, the longer the side chain. Two histidyl side chains can be seen at the top third of the molecule (lightest blue). The histidine on the right is the active-site His83, and to the left is His68. The model was generated on a Silicon Graphics Iris/4D workstation with the computer program RASTER3D written by David Bacon.

the coefficients $|F_o| - |F_c|$ and calculated phases. As the phases improved, adjustments were made to the model, and the electron density associated with most of the N-terminus became clear. Currently, after three cycles of X-PLOR refinement, the R-factor is 0.201 for data between 6.0 and 2.2 Å for which $F \geq 2\sigma(F)$. The atomic root mean square (rms) deviations from standard bond length and bond angles are 0.018 Å and 3.6°, respectively. The model includes all but the three N-terminal and one C-terminal amino acid residues. Solvent molecules have not been assigned yet. Figure 1 (bottom) shows a region of the current electron density map at 2.2-Å resolution around the active-site histidyl residue.

The coordinates have been deposited in the Brookhaven Protein Data Bank (Bernstein et al., 1977).

Results and Discussion

(A) Molecular Conformation of the IIA Domain of the Glucose Permease. The IIA domain of the glucose permease forms a predominantly antiparallel β-structure [for review, see Richardson (1981)]. Although the β-sheet hydrogen bonding is far from perfect, and some of the strand–strand interactions are missing altogether, the structure may be viewed as a β-barrel incorporating "Greek key" and "jellyroll" topological motifs. Figure 2 shows the overall three-dimensional fold of the molecule, and Figure 3, a space-filling model. Sequential numbering of the expressed domain is used, such that the active-site histidyl residue is His83. It is equivalent to His90 in the homologous IIA^{glc} (Enzyme III^{glc}) from *E. coli*. Note that when the two sequences are aligned without any deletion or insertion, the first residue in *B. subtilis* IIA^{glc} is equivalent to residue 8 in the *E. coli* protein. However, there is no sequence identity between the two up to residue 18 in the *B. subtilis* protein.

In addition to the β-strands of the barrel, there are a few short strands associated with loops which interact to form small β-sheets. There are also two short α-helics and two three-residue-long 3_{10}-helices. The precise assignment of the beginning and ends of strands and helices may be altered following the completion of the refinement. At present, secondary structure analysis using the DSSP program (Kabsch & Sander,

Table III: Structural Analysis of the Binary Comparisons of the IIA Protein Domains Shown in Figure 4[a]

	IIA^{glc}-S.t.		IIA^{nag}-E.c.		IIA^{glc}-B.s.		IIA^{bgl}-E.c.		IIA^{scr}-S.m.		P^{lac}-S.th.		P^{lac}-L.b.	
	identity[b] (%)	CS[c]	identity (%)	CS	identity (%)	CS	identity (%)	CS	identity (%)	CS	identity (%)	CS	identity (%)	CS
IIA^{glc}-E.c.	98 (169)	69	48 (155)	34	43 (156)	27	40 (147)	25	37 (159)	34	35 (151)	25	33 (133)	26
IIA^{glc}-S.t.			49 (155)	35	44 (156)	33	39 (147)	26	37 (159)	26	35 (151)	20	32 (133)	21
IIA^{nag}-E.c.					41 (160)	38	37 (168)	36	33 (162)	31	38 (150)	24	35 (155)	30
IIA^{glc}-B.s.							44 (135)	33	37 (156)	24	51 (100)	24	32 (148)	30
$IIIA^{bgl}$-E.c.									39 (168)	25	41 (159)	25	39 (125)	27
IIA^{scr}-S.m.											38 (159)	30	33 (146)	29
P^{lac}-S.th.													47 (171)	54

[a] The abbreviations are as provided in the legend to Figure 4. [b] Values in parentheses denote the number of amino acids in the segment which exhibits the indicated identity. The FASTA program (Pearson & Lipman, 1988) was used to calculate the percent identity of one protein to another. [c] Values denote the comparison scores (CS) in standard deviations that were obtained with 50 comparisons of randomized sequences of these protein segments. The RDF2 program (Pearson & Lipman, 1988) was used to calculate the comparison scores.

1983) shows the following residues to be in β-strands: 21–25, 41–47, 51–53, 58–63, 69–74, 79–83, 96–98, 105–106, 111–115, 129–133, 142–144, 149–150, and 158–160. This method of assignment is unbiased; however, it tends to somewhat underestimate the amount of secondary structure. In particular, residues 12–17 are not involved in the hydrogen bonding of the barrel but clearly adopt a β-strand conformation. Although they are not analyzed as forming a strand by the DSSP program, they are shown as such in Figure 1 (bottom). Residues that are analyzed by the DSSP program to be in helical conformation are 26–28 (3_{10}-helix), 32–35 (α-helix), 89–91 (3_{10}), and 117–123 (α-helix + 3_{10}). Three of the loops conform to the criteria of being Ω-loops (Leszczynski & Rose, 1986): Ω_1 spans residues 26–42 and contains a three-residue 3_{10}-helix and a four-residue α-helix. Ω_2 spans residues 99–112 and contains a two-residue β-strand. Ω_3 spans residues 146–157 and contains a two-residue β-strand as well. The secondary structure assignments of the protein based on NMR data have been obtained recently (Fairbrother et al., 1991). The assignments of β-strands are quite similar to those obtained from the crystal structure; however, no helices have yet been identified by the NMR work. The secondary structure assignments of the homologous Enzyme III^{glc} from *E. coli* based on NMR data have been published as well (Pelton et al., 1991). Their assignments share common features with the X-ray structure, but there are substantial differences. These include longer helical regions, an assignment of a helix which is not seen in the X-ray structure, longer β-strands, and some β-strands which are seen in the X-ray structure but are missing in the *E. coli* NMR work.

This is a single-domain protein formed with an extensive hydrophobic core containing striking clusters of phenylalanine and isoleucine residues. There are intricate hydrophobic interactions between residues remote in sequence, assuring the structural integrity of the molecule. The few hydrophilic residues found in the core adopt side-chain conformations that facilitate electrostatic interactions with main-chain atoms. Proline residues occur with unusually higher frequency (11 residues out of 162). All but one are associated with secondary structure termination and loop regions. At this stage of the refinement they all appear to adopt a trans peptide conformation.

(*B*) *Spatial Disposition of Conserved Residues.* The sequences of five PTS proteins reported to date are homologous to the *B. subtilis* IIA^{glc} domain (Meadow et al., 1990). Furthermore, the C-terminal domains of the non-PTS lactose permeases from *Streptococcus thermophilus* and *Lactobacillus bulgaricus* show remarkable sequence similarity to this class of IIA domains (Poolman et al., 1989). These sequences were aligned (Figure 4), and the phylogenetic tree revealing the degree of sequence similarities among these proteins was constructed (Table III, Figure 5). Three clusters of proteins, all sufficiently similar to assume that they are evolutionarily related, can be identified (see legend to Figure 5). These three groups agree with the evolutionary studies of the PTS permeases in general (A. Reizer et al., 1991).

The locations of conserved residues have been analyzed in the context of the crystal structure. There are a total of 28 invariant residues in the six PTS IIA domains, of which 21 are also conserved in the two non-PTS domains. Figure 6 shows the location of these residues, and Table IV summarizes the structural features relevant to each of them. Many of the conserved positions (13) are associated with the active site. Some may have a functional role, and these are discussed in more detail later. Others fulfill packing and folding requirements.

There is a group of three conserved residues remote from the active site but on the same side of the surface: Gly77, Glu79, and Asn135. Gly77 and Asn135 appear to be required to maintain structural integrity (Table IV), but there is no apparent structural reason why Glu79 should be invariant. We propose that it serves as a recognition site for one of the interacting PTS proteins, while Gly77 and Asn135 assure its precise orientation.

(*C*) *Environment of the Active Histidine.* The histidyl residue with the phosphoryl transfer function, His83, is located in a shallow depression at the C-terminus of the seventh β-strand of the barrel (Figure 3). This depression is formed by a portion of the β-sheet and the Ω_1-loop, which wraps around the side of the barrel and flanks one side of the active site (on the right in the view shown in Figures 2 and 3). A second conserved histidine, His68 (equivalent to His75 in the *E. coli* protein), is located adjacent to His83, such that its N^{ϵ} atom interacts with the N^{ϵ} atom of His83 (3.2 Å), the atom to be phosphorylated (Figure 7). Note that although nitrogen and carbon atoms cannot be discriminated within the resolution limit of the structure determination, the type of electrostatic interactions associated with these two histidine residues permits such an assignment unambiguously. Figure 5 shows the primary interactions involved: The N^{δ} atom of His83 interacts with the main-chain oxygen atom of Gly85 (2.7 Å), suggesting that the N^{δ} atom is protonated. As can be seen in Figure 3, the N^{ϵ} atom is partially exposed to solvent, consistent with it being the target for phosphorylation (Dörschug et al., 1984). The close interaction between the N^{ϵ} atoms of His83 and His68 suggests that they share a proton. However, the relative orientation of the two imidazole rings is such that the proton cannot be collinear with both N^{ϵ} atoms. Although solvent molecules have not been assigned yet, the current electron density map indicates that a solvent molecule is located close to the two histidine residues, such that it is hydrogen-bonded to both N^{ϵ} atoms. This is consistent with the nonlinearity of

```
IIA^glc E.c.    1   M G L F D K L K S L V S D D K K D T G T I E I I A P L S G E I V N I E D V P D V V F A E K I V G D G
IIA^glc S.t.    1   M G L F D K L K S L V S D D K K D T G T I E I V A P L S G E I V N I E D V P D V V F A S K I V G D G
IIA^nag E.c.  479   T P A T A A P V A K P Q A V P N A V S I A E L V S P I T G D V V A L D Q V P D E A F A S K A V G D G
IIA^glc B.s.    X                   M I A E P L Q N E I G E E V F V S P I T G E I H P I T D V P D Q V F S G K M M G D G
IIA^bgl E.c.  457   Q P A Q G A P Q E K T P E V I T P P E Q G G I C S P M T G E I V P L I H V A D T T F A S G L L G K G
IIA^scr S.m.  495   E V Q E I P E E A A S A A N K A Q V T D E V L A A P L A G E A V E L T S V N D P V F S S E A M G K G
plac    S.th. 462   E E L E H R F S V A T S E N E V K A N V V S L V T P T T G Y L V D L S S V N D E H F A S G S M G K G
plac    L.b.  455   D Q L E T Q F G Q S H A Q K P A Q A E S F T L A S P V S G Q L M N L D M V D D P V F A D K K L G D G

IIA^glc E.c.   51   I A I K P T G N K M V A P V D G T I G K I F E T N H A F S I E S D S G V E L F V H F G I D T V E L K
IIA^glc S.t.   51   I A I K P T G N K M V A P V D G T I G K I F E T N H A F S I E S D S G I E L F V H F G I D T V E L K
IIA^nag E.c.  529   V A V K P T D K I V V S P A A G T I V K I F N T N H A F C L E T E K G A E I V V H M G I D T V A L E
IIA^glc B.s. X+43   F A I L P S E G I V V S P V R G K I L N V F P T K H A I G L Q S D G G R E I L I H F G I D T V S L K
IIA^bgl E.c.  507   I A I L P S V G E V R S P V A G R I A S L F A T L H A I G I E S D D G V E I L I H V G I D T V K L D
IIA^scr S.m.  545   I A I K P S G N T V Y A P V D G T V Q I A F D T G H A Y G I K S D N G A E I L I H I G I D T V S M E
plac    S.th. 512   F A I K P T D G A V F A P I S G T I R Q I L P T R H A V G I E S E D G V I V L I H V G I G T V K L N
plac    L.b.  505   F A L V P A D G K V Y A P F A G T V R Q L A K T R H S I V L E N E H G V L V L I H L G L G T A K L N

IIA^glc E.c.  101   G E G F K R I A E E G Q R V K V G D T V I E F D L P L L E E K A K S T L T P V V I S N M D E I K E L
IIA^glc S.t.  101   G E G F K R I A E E G Q R V K V G D P V I E F D L P L L E E K A K S T L T P V V I S N M D E I K E L
IIA^nag E.c.  579   G K G F K R L V E E G A Q V S A G Q P I L E M D L D Y L N A N A R S M I S P V V C S N I D D F S G L
IIA^glc B.s. X+93   G E G F T S F V S E G D R V E P G Q K L L E V D L D A V K P N V P S L M T P I V F T N L A E G E T V
IIA^bgl E.c.  557   G K F F S A H V N V G D K V N T G D R L I S F D I P A I R E A G F D L T T P V L I S N S D D F T D V
IIA^scr S.m.  595   G K G F E Q K V Q A D Q K I K K G D V L G T F D S D K I A E A G L D N T T M F I V T N T A D Y A S V
plac    S.th. 562   G E G F I S Y V E Q G D R V E V G Q K L L E F W S P I I E K N G L D D T V L V T V T N S E K F S A F
plac    L.b.  555   G T G F V S Y V E E G S Q V E A G Q Q I L E F W D P A I K Q A K L D D T V I V T V I N S E T F A N S

IIA^glc E.c.  151   - I K L S - G S V T V G E T P V I R I K K
IIA^glc S.t.  151   - I K L S - G S V T V G E T P V I R I K K
IIA^nag E.c.  629   I I K A Q - G H I V A G Q T P L Y E I K K
IIA^glc B.s.X+143   S I K A S - G S V N R E Q E D I V K I E K
IIA^bgl E.c.  607   L P - H G - T A Q I S A G E P L L S I I R
IIA^scr S.m.  645   E T L A S - S G T V A V G D S L L E V K K
plac    S.th. 612   H L E Q K V G E K V E A L S E V I T F K K G E
plac    L.b.  605   Q M L L P I G H S V Q A L D D V F K L E G K N
```

FIGURE 4: Multiple alignment of the IIA^{glc} proteins of *E. coli* (E.c.) (De Reuse & Danchin, 1988; Saffen et al., 1987) and *S. typhimurium* (S.t.) (Nelson et al., 1984) with the IIA^{nag} domain of the *E. coli N*-acetylglucosamine permease (Peri & Waygood, 1988; Rogers et al., 1988), the recombinant IIA^{glc} protein derived from the *B. subtilis* (B.s.) glucose permease (Sutrina et al., 1990), the IIA^{bgl} domain of the *E. coli* β-glucoside permease (Schnetz et al., 1987; Bramley & Kornberg, 1987), the IIA^{scr} domain of the *Streptococcus mutans* (S.m.) sucrose permease (Sato et al., 1989), and the two IIA-like domains associated with the lactose:galactose antiporters (P^{lac}) of *Streptococcus thermophilus* (S.th.) (Poolman et al., 1989) and *Lactobacillus bulgaricus* (L.b.) (Leong-Morgenthaler et al., 1991). Residues conserved in all proteins are shown in boldface type. The first amino acid of the recombinant IIA^{glc} protein derived from the *B. subtilis* glucose permease is labeled X since the amino acid sequence of this permease at its N-terminus has yet to be determined (Gonzy-Treboul et al., 1989).

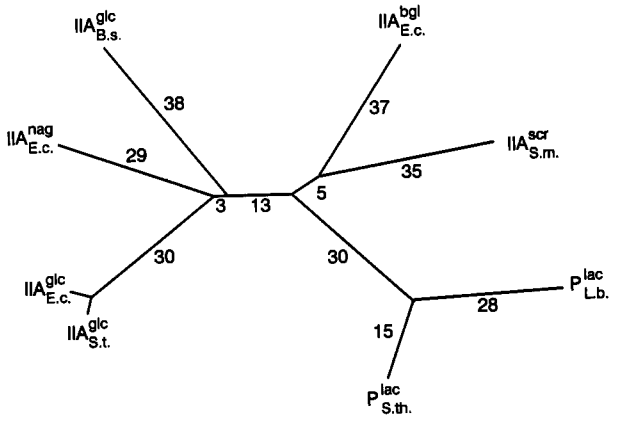

FIGURE 5: Phylogenetic tree for the eight sequenced members of the family of IIA^{glc} proteins and IIA^{glc}-like protein domains. Relative evolutionary distances are given adjacent to the branches. The programs of Doolittle and Feng (1990) and Feng and Doolittle (1990) were used to calculate relative distances. The abbreviations are as provided in the legend to Figure 4. Three main clusters are apparent: (a) $IIA^{glc}_{E.c.}$, $IIA^{glc}_{B.s.}$, $IIA^{glc}_{S.t.}$, and $IIA^{nag}_{E.c.}$; (b) $IIA^{bgl}_{E.c.}$ and $IIA^{scr}_{S.m.}$, and (c) $P^{lac}_{L.b.}$ and $P^{lac}_{S.th.}$.

the interhistidine hydrogen bond. The N^{δ} atom of His68 interacts with the O^{γ} atom of Thr66 (2.8 Å), a conserved residue in all the known IIA domains. Since the threonine O^{γ} atom can be either a proton donor or a proton acceptor, the N^{δ} atom may be either protonated or deprotonated. If protonated, the histidyl pair would be positively charged. Such two charged states may have a functional role (see section G). The crystal structure reflects the resting state of the protein. In the activated state the N^{ϵ} atom of His83 should be deprotonated, ready for a nucleophilic attack on phospho-HPr; thus the proton may reside on His68. The relatively long distance and the distorted geometry of the hydrogen bond between the two imidazole rings suggest that the resting-state conformation seen in the crystal structure is close to the activated state.

To the best of our knowledge, there is only one more protein of known crystal structure with two neighboring histidine residues in the active site: yeast phosphoglycerate mutase, which catalyzes the interconversion of 2- and 3-phosphoglycerate (Winn et al., 1981). The structure has been determined at 2.8-Å resolution but is not well refined. Inspection of the coordinates that have been deposited in the Brookhaven Protein Data Bank (accession number 3PGM, Bernstein et al., 1977) shows that the two imidazole rings in the active site are stacked parallel to each other. An arginine and two glutamate residues are also involved. Thus, despite the analogy in function (the transfer of a phosphoryl group) this arrangement is completely different than the one seen in the crystal structure of the IIA domain of the glucose permease. Moreover, the disposition of the active-site residues of phosphoglycerate mutase cannot be considered reliable; each of the histidine side-chains makes much too close (2.0 Å) contacts with main-chain atoms of the following residue. Further refinement of the mutase structure is needed before a meaningful comparison can be made.

The mechanism of catalysis by ribonuclease has been studied [see, for example, Anslyn and Breslow (1989)]. Two histidine residues are involved in catalysis. However, their relative

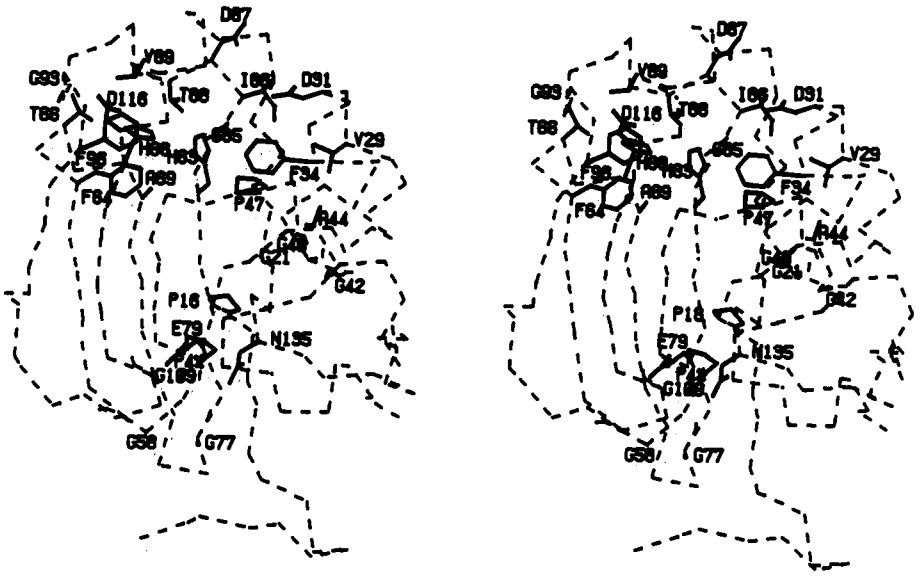

FIGURE 6: Stereoscopic representation of the location of conserved amino acid residues from six sequences of IIA domains in the structure of the *B. subtilis* IIA^{glc}. Virtual bonds between α-carbon atoms are shown in broken lines and the side-chain bonds in continuous lines. The conserved residues are labeled.

Table IV: Proposed Roles for the Conserved Residues in the IIA Domains

residue	location	role
Pro18	β-strand termination, protein core	packing requirements; associated with conserved Pro55 and a cluster of three Phe; folds such that the O^{γ} atom of the adjacent Ser17 interacts with the main-chain nitrogen atom of residue 19 (Asx turn)
Gly21	β-strand initiation	packing and folding requirements; the main-chain ϕ,ψ dihedral angles are +160°, −153°, a sterically strained conformation for a β-carbon-containing residue; the packing is such that there is no space for a residue with a β-carbon atom
Val29	Ω_1-loop	packing requirements; in a hydrophobic environment that defines the association of the loop with the rest of the structure; some of the interacting hydrophobic groups are also conserved
Asp31	Ω_1-loop closure to the active site	may have a functional role (see section E)
Phe34	Ω_1-loop closure to the active site	may have a functional role (see section D)
Gly40	β-strand initiation	folding and packing requirements; ϕ,ψ = 165°, 173°, a sterically strained conformation for a β-carbon-containing residue; a β-carbon atom would make too-close contacts with main-chain atoms of a neighboring residue
Ala44	β-strand	packing requirements; no space for a larger residue
Pro47	β-strand termination	hydrophobic core, packing against Phe84; should be replaceable
Pro55	β-strand termination	pseudo-2-fold symmetry with conserved Pro18, with a similar role, including the forming of an Asx turn by Ser54
Gly58	β-strand initiation	pseudo-2-fold symmetry with conserved Gly21, with a similar structural role
Phe64	active site	conserved only in the sequences of PTS IIA domains; thus, it may have a functional role (see section D)
Thr66	active site	electrostatic interaction with the active-site His68
His68	active site	electrostatic interaction with the catalytic His83
Ala69	active site	packing requirements; packs against the active-site His68 and Phe64; conserved in all sequences of the PTS proteins
Gly77	reverse turn	associated with a second cluster of conserved residues that may be important for protein–protein interaction
Glu79	β-strand initiation	exposed to solvent on the N-terminus of the strand that leads to the active-site His83; conserved in all PTS IIA domains and may have a role in domain recognition within the permease
His83	active site	target residue for phosphorylation
Gly85	active site	packing requirements; no space for a β-carbon atom; its main-chain oxygen atom interacts with His83 N^{δ} atom
Ile86	close to the active site	conserved in seven out of eight sequences; its role is not clear
Asp87	close to the active site	conserved in all sequences of the PTS proteins; may have a functional role (see section E)
Thr88	active site	hydrogen-bonded to the active-site Gly85, fixing its orientation relative to His83
Val89	active site	exposed hydrophobic residue associated with the active site; may have a role in protein–protein recognition
Gly93	reverse turn	folding requirements; ϕ,ψ = +85°, −6°, a sterically strained conformation for a β-carbon-containing residue
Phe96	active site	packing requirements; packs against His68 main chain
Gly109	β-strand termination	folding requirements; ϕ,ψ = +106°, −19°, a sterically strained conformation for a β-carbon-containing residue
Asp116	terminates β-strand, initiates 3_{10}-helix	no apparent role; should be replaceable at least by Asn
Asn135	β-strand	folding requirements; the side chain is hydrogen-bonded to the main-chain nitrogen atom of conserved Glu78 and to the main-chain oxygen of conserved Gly77; possibly a second protein–protein recognition site

disposition does not resemble that of the histidine residues in the IIA^{glc} domain, they do not interact with each other, and they are not ligands of the pentacoordinated phosphorus intermediate.

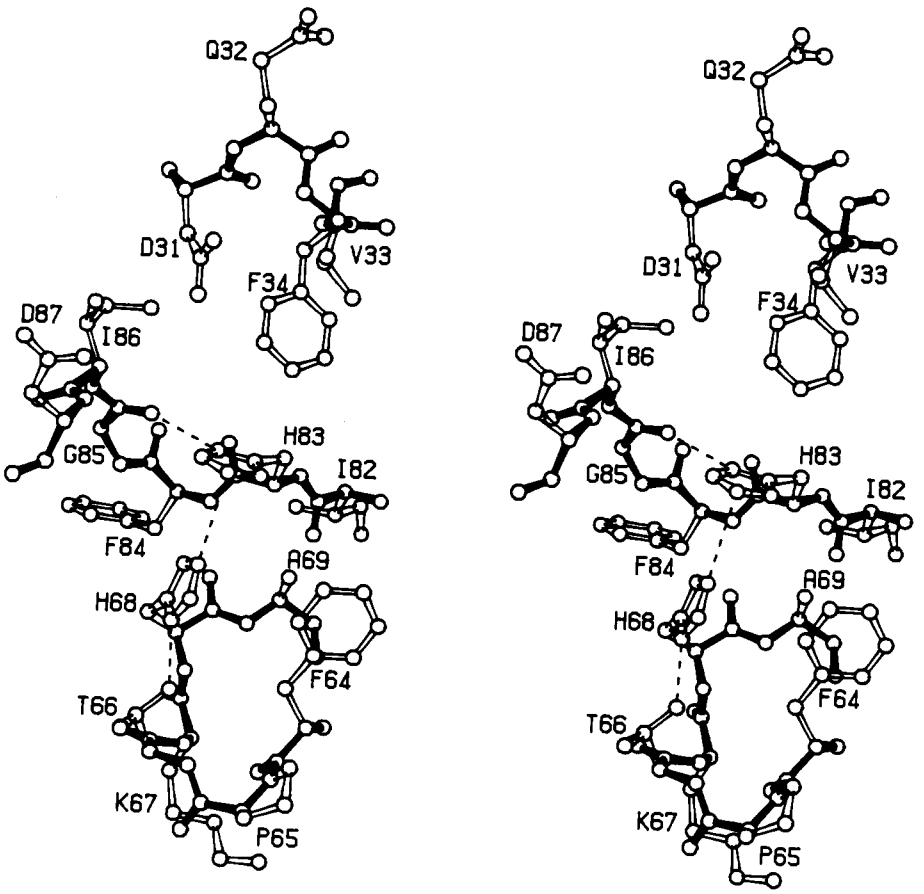

FIGURE 7: Stereoscopic view of the active-site region of the IIA^{glc} enzyme. Bonds between main-chain atoms are filled and those between side-chain atoms are open. Important stabilizing interactions are shown in broken lines. The N^{δ} of His83 interacts with the main-chain O atom of Gly85. The N^{ϵ} atom of His83 interacts with the N^{ϵ} atom of His68. The N^{ϵ} atom of His68 interacts with the O^{γ} atom of Thr66.

(*D*) *Hydrophobic Nature of the Surface Around the Active-Site Histidine.* The surface around the two histidyl residues is enriched with hydrophobic residues (Figure 3), suggesting that these may be important for protein–protein recognition either by HPr or by the IIB domain of the permease. In particular, the three hydrophobic residues, Val33, Met38, and Met39, which are located on the Ω_1-loop, form a ridge to the right of His83, in the orientation shown in the figure. These are always hydrophobic residues in the known IIA domains.

The two active-site histidine residues are flanked by two phenylalanine residues which are conserved in all the IIA sequences. These make van der Waals interactions with the histidyl pair, further assuring their precise relative orientation (Figure 7). Phe34, adjacent of His83, is located on the Ω_1-loop and is mostly buried by the hydrophobic patch (Figure 3). From the other side, Phe64, adjacent to His68, is exposed to solvent. The four aromatic rings make face-to-edge pairwise ring interactions (James & Sielecki, 1983; Burley & Petsko, 1985), in contrast to the stacked packing that has been reported to be common for phenylalanine–histidine pairs (Burley & Petsko, 1986). Since Phe64 is an exposed residue, it may be important for the interaction with HPr and/or the IIB domain. The proximity of Phe34 to His83 and its burial by the hydrophobic patch of the Ω_1-loop suggest that it may play a functional role, the nature of which is not clear.

(*E*) *Proposed Functional Role for Two Conserved Aspartates.* There are two aspartyl residues that are conserved in the PTS IIA domains: Asp31 and Asp87. They are located about 7 Å away from His83, with their carboxylate moieties oriented toward each other 4.7 Å apart across a narrow groove (the red side chains shown in the top right side of Figure 3 and in Figure 7). This is an unusual electrostatic arrangement for two negatively charged residues, considering the high pH of the crystals (8.0). These two aspartates are too far from His83 to affect the phosphoryl transfer directly. Rather, they may form a binding site for a positively charged residue associated with the active site of either HPr or Enzyme IIB (Arg17 has been proposed to be associated with the active site of HPr; Klevit & Waygood, 1986). Such an interaction would alter the electrostatic environment of the phosphorylated species and facilitate phosphoryl transfer.

The aspartate equivalent to Asp87 in the homologous β-glucoside permease of *E. coli* has been replaced by an alanyl residue by site-directed mutagenesis (Schnetz et al., 1990). The decrease in the catalytic rate of this mutant relative to the wild-type protein has been interpreted as evidence that the aspartyl side chain plays a catalytic role. The spatial position of Asp87 indicates that the replacement by an alanyl residue is structurally conservative and should not destabilize the protein, when in principle could also affect catalysis. Thus this mutagenesis result is consistent with the three-dimensional structure.

(*F*) *The N-Terminus.* The 13 N-terminal amino acid residues form part of the Q-linker region between domains IIA and IIB of the permease. They fold somewhat independently from the rest of the structure, forming a hairpin loop that interacts only marginally with the rest of the structure, with the first three residues disordered in the current model (Figure 2). Glu4 interacts with Arg58 and Arg105, and Glu12 interacts with Lys159 close to the C-terminus. These interactions are too far to be considered salt bridges. It has been proposed that Q-linkers are structurally flexible. However, in this crystal structure they have a unique conformation,

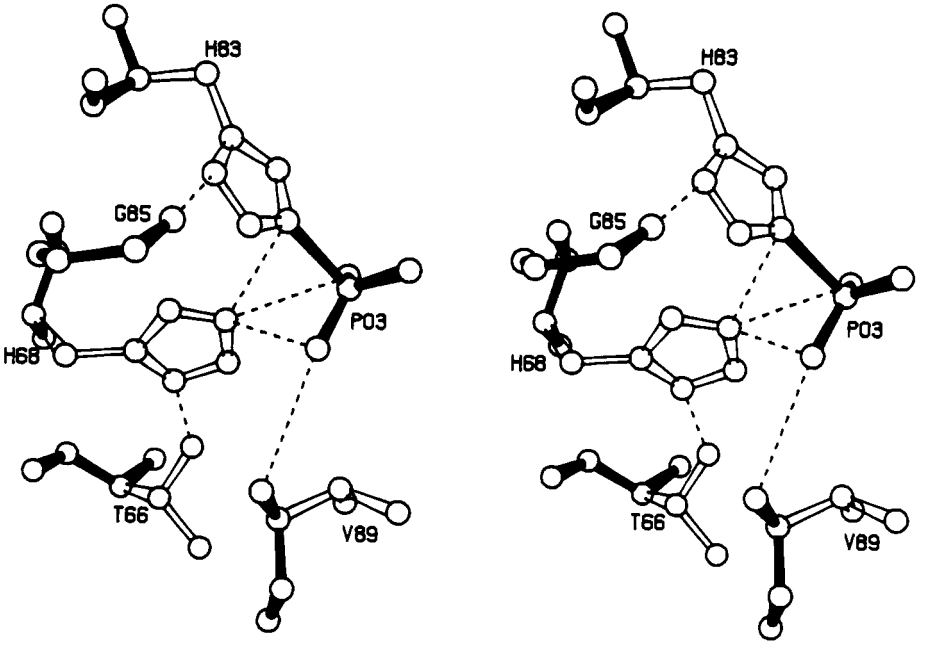

FIGURE 8: Stereoscopic view of the model of the phosphorylated histidine. Bonds between main-chain atoms are filled and those between side-chain atoms are open. Important stabilizing interactions are shown in broken lines. The phosphoryl oxygen atoms interact with the His68 N^{ϵ} atom and with the main-chain nitrogen atom of Val89.

although the crystallographic temperature factors of residues 4–7 are elevated ($B \sim 30$–40 Å^2). There are only a few crystal packing contacts between this segment and other symmetry-related molecules; thus the conformation of the N-terminus is not an artifact of the crystal environment. The conformation seen may not have physiological relevance, though, since a large portion of the Q-linker is missing, as is the entire IIB domain. The interaction with these and with the membrane could induce a different conformation of the N-terminal segment.

The length of the *B. subtilis* N-terminal polypeptide is identical to that of III^{glc}_{fast} from *E. coli* (Meadow et al., 1986), and both are eight residues shorter than III^{glc}_{slow}. The III^{glc}_{fast} is a proteolytic cleavage product of the intact protein, III^{glc}_{slow}. It is always isolated with the intact protein and is identified by its more rapid migration on nondenaturing polyacrylamide gels. Whereas the function of the III^{glc}_{fast} as a phosphoryl donor is impaired relative to the intact protein, the *B. subtilis* enzyme is fully active and can also replace the *E. coli* enzyme. The reason for this difference is not clear. The crystal structure indicates that the N-terminus is too remote from the active site to interact with catalytic residues and be directly involved in phosphoryl transfer (Glu4 is 30 Å away from the active site). Inspection of the structure shows that substantial parts of the molecule would be required to unfold for such interactions to take place. It is more likely that differences in sequence between the N-termini of the *B. subtilis* and the *E. coli* proteins, such as the charge balance or the distribution of hydrophobic residues, reflect structural differences that destabilize the interaction of the III^{glc}_{fast} with the rest of the permease and/or the membrane.

Schnetz et al. (1990) prepared mutants of the β-glucoside permease from *E. coli* in which the C-terminal arginine was replaced by an aspartate or truncated (equivalent to the C-terminal lysine in the IIA^{glc} of *B. subtilis*). They interpreted the decrease in the catalytic rates as indicating that the C-terminus plays a mechanistic role in the phosphoryl transfer. The C-terminus is exposed to solvent with the C-terminal lysine disordered in the crystal structure. Truncation or replacement of the lysine by another hydrophilic residue should not, therefore, destabilize the protein. However, the kinetic data are not corroborated by the structural information. The C-terminus is remote from the active site, some 30 Å away from His83, and cannot be directly involved in the phosphorylation. In fact, it is close to the N-terminal region. We propose that, like the N-terminus, the C-terminus may play a role in protein–protein association, possibly with the other domains of the permease or with the membrane, since it is difficult to envision a small protein such as HPr spanning the whole of the surface from His83 to the C-terminus.

(G) A Model of the Phosphorylated IIA Domain. It is possible to model the phosphorylated state of the IIA domain of the permease such that there are no close contacts. The phosphoryl group was built so that the phosphorus atom is in the plane of the imidazole ring of His83 (Figure 8). The model shows that the two of the oxygen atoms of the negatively charged phosphoryl group can interact with the N^{ϵ} atom of His68 (2.8 Å) as well as with the main-chain nitrogen of Val89 (3.1 Å). A protonated His68 may therefore play a role in stabilizing the phospho-IIA state.

The pK values of the two histidyl residues have not been reported for any of the IIA domains that are homologous to the *B. subtilis* domain. NMR studies of the IIA^{lac} from *Staphylococcus aureus*, a protein whose sequence is not related to the *B. subtilis* IIA^{glc}, showed that all four histidyl residues in that protein have acidic pK values around 6 (Kalbitzer et al., 1981). Upon phosphorylation, the pK of the remaining proton of the catalytic histidyl is 8.6. Although the disposition of the active-site residues in the *B. subtilis* IIA^{glc} may be quite different, the hydrogen-bonding network suggests that there, as well, a proton is located on the N^{δ} atom of the phosphorylated His83. Whether the pK of the adjacent His68 is altered by the phosphorylation is yet to be determined. Nevertheless, the hydrogen-bonding network in which His68 interacts with the O^{γ} atom of a threonine residue shows that His68 could become protonated on both nitrogens.

It has been shown by site-directed mutagenesis that His75 in the *E. coli* III^{glc} can be replaced by a glutamine (Presper et al., 1989) and that the equivalent His68 in the *B. subtilis* IIA^{glc} can be replaced by an alanine (J. Reizer et al., 1991),

resulting in defective proteins that can be phosphorylated by HPr but cannot perform the phosphoryl transfer to IIB^{glc}. Thus, it is clear that the mechanisms of accepting and donating a phosphoryl group must differ, suggesting that HPr and the IIB domain offer different surfaces for the interaction with the IIA domain. On the basis of this information, Presper et al. (1989) proposed that the phosphoryl group may migrate from the catalytic histidine to the adjacent histidine. The relative positions of the two histidines, with the modeled phosphoryl group close to both, implies that the reaction proceeds via the adjacent associative pathway [for review, see Knowles (1980)]. All associative pathways involve pentacoordinated intermediates or transition states having trigonal bipyramidal geometry, and the adjacent course is accompanied by a pseudorotation, with retention of the stereochemical configuration at the phosphorus. The pentacoordinated intermediate would thus have one histidyl in an apical position, and the other would be equatorial. The N^{ϵ} of His68 would be deprotonated. The relative energetics of imidazole in the equatorial versus apical positions in the trigonal bipyramidal intermediate is not known, though.

Begley et al. (1982) have shown that, consistent with the five steps of phosphoryl transfer from PEP to the sugar, each of which is thought to proceed via the associative pathway with inversion of configuration at the phorphorus, there is an overall inversion of configuration. Since the migration step proposed by Presper et al. (1989) results in retention of configuration at the phosphorus, this additional step does not contradict the finding of Begley et al. Thus, there is no experimental evidence to exclude the possibility of migration.

We propose another possible mechanistic role for His68, which differentiates between histidine and glutamine residues without the need to invoke an additional phosphoryl transfer step: The overall shape of the active site of the IIA domain of the glucose permease and the hydrophobic patch that surrounds His83 indicate that while being transferred the negatively charged phosphoryl group is desolvated. Hence, the electrostatic interactions within the transient complexes are extremely important. The only significant electrostatic interactions with the IIA^{glc} molecule available for the phosphoryl group are those with the side chain of His68 and the NH of Val89. Other interactions have to involve the second protein partner in each of the transfer steps. The mutagenesis results show that the electrostatic interactions with His68 are apparently not essential for the interaction with HPr, implying that the negative charge of the phosphoryl group buried in the transient complex is balanced by the surrounding dipoles and positive charges, including those of HPr. Apparently, this is not the case in the IIA–IIB complex without His68. In contrast to a glutamine, a histidine can be positively charged. Both the neutral and positively charged states are consistent with the crystal structure. We therefore propose that the active site of the IIB domain may involve a carboxylate charge or some negative environment due to carbonyl groups, perhaps to facilitate the interaction with the incoming sugar, such that His68 must be protonated for a productive IIA–IIB interaction. A glutamine residue cannot be protonated; thus the docking with the IIB is unfavorable and the phosphoryl transfer is inhibited. The confirmation of this, or any other proposal, awaits the high-resolution structure determination of HPr and the IIB domain of the permease.

Acknowledgments

We thank John Moult, Walt Stevens, Gary Gilliland, and Tom Poulos for many helpful discussions and Erik Velapoldi for help in the purification of the protein. Certain commercial equipment, instruments, and materials are identified in this paper in order to specify the experimental procedure as completely as possible. In no case does such identification imply a recommendation or endorsement by the National Institute of Standards and Technology, nor does it imply that the material, instrument, or equipment identified is necessarily the best available for the purpose.

References

Anslyn, E., & Breslow, R. (1989) *J. Am. Chem. Soc. 111*, 4473–4482.

Begley, G. S., Hansen, D. E., Jacobson, G. R., & Knowles, J. R. (1982) *Biochemistry 21*, 5552–5556.

Bernstein, F. C., Koetzle, T. F., Williams, G. J. B., Meyer, E. F., Jr., Brice, M. D., Rodgers, J. R., Kennard, O., Shimanouchi, T., & Tasumi, M. (1977) *J. Mol. Biol. 112*, 535–542.

Blow, D. M., & Crick, F. H. C. (1959) *Acta Crystallogr. 12*, 794–802.

Blundell, T. L., & Johnson, L. N. (1976) *Protein Crystallography*, Academic Press, London.

Bramley, H. F., & Kornberg, H. L. (1987) *J. Gen. Microbiol. 133*, 563–573.

Brünger, A. T., Kuriyan, J., & Karplus, M. (1987) *Science 235*, 458–460.

Burley, S. K., & Petsko, G. A. (1985) *Science 229*, 23–28.

Burley, S. K., & Petsko, G. A. (1986) *FEBS Lett. 203*, 139–143.

Dean, D. A., Reizer, J., Nikaido, H. & Saier, M. H., Jr. (1990) *J. Biol. Chem. 265*, 21005–21010.

De Reuse, H., & Danchin, A. (1988) *J. Bacteriol. 170*, 3827–3837.

Deutscher, J., Kessler, U., Alpert, C. A., & Hengstenberg, W. (1984) *Biochemistry 23*, 4455–4460.

Dickerson, R. E., Weinzierl, J. E., & Palmer, R. A. (1968) *Acta Crystallogr. B24*, 997–1003.

Doolittle, F. R., & Feng, D.-F. (1990) *Methods Enzymol. 183*, 659–669.

Dörschug, M., Frank, R., Kalbitzer, H. R., Hengstenberg, W., & Deutscher, J. (1984) *Eur. J. Biochem. 144*, 113–119.

El-Kabbani, O. A. L., Waygood, E. B., & Delbaere, L. T. J. (1987) *J. Biol. Chem. 262*, 12926–12929.

Fairbrother, W. J., Cavanagh, J., Dyson, H. J., Palmer, A. G., Sutrina, L. S., Reizer, J., Saier, M. H., Jr., & Wright, P. E. (1991) *Biochemistry 30*, 6896–6907.

Feng, D.-F., & Doolittle, F. R. (1990) *Methods Enzymol. 183*, 375–387.

Furey, W., & Swaminathan, S. (1990) 14th American Crystallographic Association Meeting, PA33.

Gênovésio-Taverne, J.-C., Sauder, U., Pauptit, R. A., Jansonius, J. N., & Erni, B. (1990) *J. Mol. Biol. 216*, 515–517.

Gonzy-Treboul, G., & Steinmetz, M. (1987) *J. Bacteriol. 169*, 2287–2290.

Gonzy-Treboul, G., Zagorec, M., Rain-Guion, M. C., & Steinmetz, M. (1989) *Mol. Microbiol. 3*, 103–112.

Howard, A. J., Gilliland, G. L., Finzel, B. C., Poulos, T., Ohlendorf, D. O., & Salemme, F. R. (1987) *J. Appl. Crystallogr. 20*, 383–387.

James, M. N. G., & Sielecki, A. R. (1983) *J. Mol. Biol. 163*, 299–361.

Jones, T. A. (1982) in *Computational Crystallography* (Sayre, D., Ed.) pp 303–317, Oxford, University Press, London and New York.

Kabsch, W., & Sander, C. (1983) *Biopolymers 22*, 2577–2637.

Kalbitzer, H. R., Deutscher, J., Hengstenberg, W., & Rösch, P. (1981) *Biochemistry 20*, 6178–6185.

Kapadia, G., Reizer, J., Sutrina, S. L., Saier, M. H., Jr., Reddy, P., & Herzberg, O. (1990) *J. Mol. Biol. 211*, 1–2.
Kapadia, G., Chen, C. C. H., Reddy, P., Saier, M. H., Jr., Reizer, J., & Herzberg, O. (1991) *J. Mol. Biol.* (in press).
Klevit, R. E., & Waygood, E. B. (1986) *Biochemistry 25*, 7774–7781.
Knowles, J. R. (1980) *Annu. Rev. Biochem. 49*, 877–919.
Leong-Morgenthaler, P., Zwaheln, M. C., & Hottinger, H. (1991) *J. Bacteriol. 173*, 1951–1957.
Leszczynski, J. F., & Rose, G. D. (1986) *Science 234*, 849–855.
Meadow, N. D., Coyle, P., Komoryia, A., Anfinsen, C. B., & Roseman, S. (1986) *J. Biol. Chem. 261*, 13504–13509.
Meadow, N. D., Fox, D. K., & Roseman, S. (1990) *Annu. Rev. Biochem. 59*, 497–542.
Nelson, S. O., Schuitema, A. R. J., Benne, R., van der Ploeg, L., Pleiter, J. J., Aan, F., & Postma, P. W. (1984) *EMBO J. 3*, 1587–1593.
Pearson, W. R., & Lipman, D. J. (1988) *Proc. Natl. Acad. Sci. U.S.A. 85*, 2444–2448.
Pelton, J. G., Torchia, D. A., Meadow, N. D., Wong, C.-Y., & Roseman, S. (1991) *Proc. Natl. Acad. Sci. U.S.A. 88*, 3479–3483.
Peri, K. G., & Waygood, E. B. (1988) *Biochemistry 27*, 6054–6061.
Poolman, B., Royer, T. J., Mainzer, S. F., & Schmidt, B. F. (1989) *J. Bacteriol. 171*, 244–253.
Postma, P. W., & Lengeler, J. W. (1985) *Microbiol. Rev. 49*, 232–269.
Powell, M. J. D. (1977) *Math. Programming 12*, 241–254.
Presper, K. A., Wong, C.-Y., Liu, L., Meadow, N. D., & Roseman, S. (1989) *Proc. Natl. Acad. Sci. U.S.A. 86*, 4052–4055.
Reizer, A., Pao, G. M., & Saier, M. H., Jr. (1991) *J. Mol. Evol.* (in press).
Reizer, J., Saier, M. H., Jr., Deutscher, J., Grenier, F., Thompson, J., & Hengstenberg, W. (1988) *CRC Crit. Rev. Microbiol. 15*, 297–338.
Reizer, J., Sutrina, S. L., Wu, L.-F., Deutscher, J., & Saier, M. H., Jr. (1991) *J. Biol. Chem.* (submitted for publication).
Richardson, J. (1981) *Adv. Protein Chem. 34*, 167–339.
Rogers, M. J., Ohgi, T., Plumbridge, J., & Söll, D. (1988) *Gene 62*, 197–207.
Saffen, D. W., Presper, K. A., Doering, T. L., & Roseman, S. (1987) *J. Biol. Chem. 262*, 16241–16253.
Saier, M. H., Jr. (1985) *Mechanisms and Regulation of Carbohydrate Transport in Bacteria*, Academic Press, New York.
Saier, M. H., Jr., & Reizer, J. (1990) *Res. Microbiol. 141*, 1033–1038.
Sato, Y., Poy, F., Jacobson, G. R., & Kuramitsu, H. K. (1989) *J. Bacteriol. 171*, 263–271.
Schevitz, R. W., Podjarny, A. D., Zwick, M., Hughes, J. J., & Sigler, P. B. (1981) *Acta Crystallogr. A37*, 669–677.
Schnetz, K., Toloczyki, C., & Rak, B. (1987) *J. Bacteriol. 269*, 2579–2590.
Schnetz, K., Sutrina, S. L., Saier, M. H., Jr., & Rak, B. (1990) *J. Biol. Chem. 265*, 13464–13471.
Sutrina, S. L., Reddy, P., Saier, M. H., Jr., & Reizer, J. (1990) *J. Biol. Chem. 265*, 18581–18589.
Wang, B. C. (1985) in *Methods in Enzymology* (Wyckoff, H. W., Hirs, C. H. W., & Timasheff, S. N., Eds.) Vol. 115, Part B, pp 90–112, Academic Press, New York.
Winn, S. J., Watson, H. C., Harkins, R. N., & Fothergill, L. A. (1981) *Philos. Trans. R. Soc. London B293*, 121–130.
Wittekind, M., Reizer, J., Deutscher, J., Saier, M. H., Jr., & Klevit, R. E. (1989) *Biochemistry 28*, 9908–9912.
Wittekind, M., Reizer, J., & Klevit, R. E. (1990) *Biochemistry 29*, 7191–7200.
Wootton, J. C., & Drummond, M. H. (1989) *Protein Eng. 2*, 535–543.